Journal of Applied Polymer Science

Hg(II) Removal from HCl Solutions Using a Tetraalkylphosphonium Ionic Liquid Impregnated Onto Amberlite XAD-7

Ricardo Navarro,[1] Janette Alba,[1] Imelda Saucedo,[1] Eric Guibal[2]

[1]División de Ciencias Naturales y Exactas, Departamento de Química, Universidad de Guanajuato, Cerro de la Venada s/n. Pueblito de Rocha, C.P. 36040 Guanajuato, Gto, Mexico

[2]Centre des Matériaux des Mines d'Alès. Pôle "Matériaux Polymères Avancés. Axe "Biopolymères, Conditionnement et Interfaces". Ecole des Mines d'Alès. 6 Avenue de Clavières, 30319 Alès Cedex, France

Correspondence to: R. Navarro (E-mail: navarrm@ugto.mx)

ABSTRACT: Extractant impregnated resins (EIRs) were prepared by impregnation of Amberlite XAD-7 with tetraalkylphosphonium chloride ionic liquid (IL). The EIRs were tested for the sorption of Hg(II) in HCl solutions. Mercury is bound on the EIR through an ion exchange mechanism involving chloroanionic species and the IL. The effect of HCl concentration and IL content is studied and the sorption isotherms are obtained in 1 M HCl solutions: the sorption capacity linearly increases with IL loading up to 100 mg Hg L^{-1}. A little fraction of the IL immobilized on the resin (about 40 mg IL g^{-1}) is tightly bound to the polymer limiting its reactivity with metal ions. The uptake kinetics are mainly controlled by intraparticle diffusion. At high IL loading the kinetics are slowed down, while the temperature has a limited impact. Nitric acid can be used for desorbing mercury and recycling the EIR for at least five cycles. © 2014 Wiley Periodicals, Inc. J. Appl. Polym. Sci. **2014**, *131*, 41086.

KEYWORDS: adsorption; functionalization of polymers; ionic liquids; resins; separation techniques

Received 23 February 2014; accepted 28 May 2014
DOI: 10.1002/app.41086

INTRODUCTION

The discharge of metal ions to the environment (wastewater from mining and industry) is strictly controlled. The regulations are becoming more and more stringent leading to the development of new processes for their elimination from wastewater. The metal ions are retaining a great attention due to their accumulative effect in the food chain. The example of mercury is illustrative of these hazards; and the Minamata contamination in Japan clearly showed the dramatic effect that the combined effects of toxicity and accumulation in food chain can cause on human health. Conventional processes such as precipitation,[1] adsorption and biosorption,[2–7] ion exchange or chelating resins,[7–12] solvent extraction,[13,14] membranes,[15–17] and so forth, frequently meet technical limitations (to reach regulation levels) or economic requirements (excessive cost for large scale applications). As far as possible it is preferable recovering these metals at the source rather than after dilution and mixing with other types of water streams. The treatment of concentrated solutions may require adjusting the process to drastic conditions such as the presence of several metals and/or strongly acidic solutions, for which conventional systems can be inappropriate. There is still a need for alternative and new sorption systems for the treatment of this kind of effluents. Extractant impregnated resins (EIRs) have retained a great attention.[18–20] They combine the easy management of solid sorbents, the high efficiency and selectivity of extractants and the extractant retention and confinement associated with the resin support (limiting the main drawback of solvent extraction, which consists in extractant dispersion and loss in the aqueous phase). A new generation of extractants has been recently tested for the recovery of metal ions in solvent extraction: ionic liquids (ILs) are characterized by very low vapor pressure (which limits solvent loss by evaporation and reduces fire and explosion hazard in their use and processing), and readily tunability (in relation with the great diversity of organic cation and organic or inorganic anions that can be associated).[20–22] Though most of the articles published on metal sorption using ILs concern imidazolium-based ILs,[20] recently a series of studies have focused on ILs bearing phosphonium cations for the recovery Zn(II), Pd(II), Pt(IV), or Fe(III)/Ni(II).[23–26] These extractants have also been used for the synthesis of hybrid sorbents associating the IL and a support such as silica,[27] synthetic resin,[28–34] biopolymer.[35–40] The immobilization may proceed by (a)

Additional Supporting Information may be found in the online version of this article.

Table I. Characteristics of Amberlite XAD-7 Resin[30]

Composition of the resin	Polyacrylic acid ester ($[CH_2\text{-}CH(COOR)]_n$)
Type of resin	Nonionic, moderately hydrophilic porous polymer
Particle size	250–850 μm (20/60 mesh)
Pore diameter	80–85 Å
Specific surface area	450 $m^2\ g^{-1}$
Porosity	0.55
Pore volume	0.97–1.14 $cm^3\ g^{-1}$
Skeletal density	1.24 g cm^{-3}

impregnation of the support with the IL diluted in an appropriate solvent followed by the evaporation of the solvent (case of synthetic resins, e.g.), or by (b) encapsulation (case of biopolymer or synthetic polymers).[37,40,41]

The present study is part of a larger investigation performed on the immobilization of Cyphos ILs (tetraalkylphosphonium ILs) using the impregnation and encapsulation methods for the preparation of new EIRs and their testing of the sorption of a series of metal ions forming chloroanionic species in HCl solutions. This study will be compared with previous results obtained on Hg(II) sorption using Cyphos IL 101 immobilized in alginate capsules.[37] The objective will be to evaluate the contribution of mass transfer properties (in relation with the effect of polymer matrix) on uptake kinetics and sorption capacities. Previous studies have pointed out the importance of metal speciation on the optimization of sorption. This study also contributes to demonstrate the importance of this critical parameter.

The first part of the study investigates the effect of both HCl concentration and IL loading on Hg(II) extraction efficiency with the objective of determining the impact of metal speciation, and the binding mechanism involved in metal uptake. The influence of IL loading on sorption isotherms allows establishing the stoichiometric ratio between the IL and Hg(II). In a second part of the study, the uptake kinetics are performed with a special attention paid to the effects of agitation speed, IL loading and temperature on kinetic profiles. This section contributes to evaluating the limiting steps (diffusion mechanisms). Finally, the desorption of the EIR after metal binding is investigated with the double objective of metal recovery and resin recycling.

EXPERIMENTAL

Materials

Amberlite XAD-7 was supplied by Sigma-Aldrich (Saint-Louis). The main properties of this resin are reported in Table I. The resin was conditioned by the supplier with NaCl and Na_2CO_3 to retard bacterial growth. It was necessary to clean it to remove salts and monomeric material present on the resin. The resin was therefore put into contact with ketone for 24 h at 25°C. After filtration under vacuum to remove excess ketone, the resin was rinsed with demineralized water. Then, it was washed with nitric acid (0.1*M*) for 24 h. The resin was filtered under vacuum and then rinsed with demineralized water to constant pH. Finally, the resin was put into contact with ketone for 12 h before being filtered under vacuum and dried in a rotavapor at 50°C. Cyphos®IL 101 was kindly supplied by Cytec (Canada). This is a phosphonium salt (tetradecyl(trihexyl)phosphonium chloride, $[P R_3R']^+ Cl^-$). Hg(II) solution were prepared from $HgCl_2$ (Karal, México) and dithizone solution from 1000 mg L^{-1} dithizone solution in chloroform (Hycel). Other reagents (salts, acids, etc) were analytical grade and supplied by KEM (Mexico). Standard metal solutions were supplied by Perkin Elmer.

Resin Impregnation

In the present work, the extractant was immobilized on the resin by a physical technique. The impregnation was performed using the so-called dry incipient method by contact of 5 g of conditioned Amberlite XAD-7 with 25 mL of ketone for 24 h. Varying amounts of Cyphos®IL 101 diluted in ketone (0.5*M*) were added to resin slurry for 24 h, under agitation. The solvent was then slowly removed by evaporation in a rotavapor. The amount of extractant immobilized on the resin (q_{IL}) was quantified by the following procedure. A known amount of impregnated resin (250 mg) was mixed with methanol (5 mL) for 24 h to dissolve the extractant and the solvent was separated from the resin by decantation. This washing treatment was performed twice. Finally, the resin was dried at 50°C for 24 h for complete evaporation of solvent. The mass difference ($M_{\text{Cyphos IL 101}}$) between impregnated ($M_{\text{XAD-7/Cyphos IL 101}}$) and washed resin ($M_{\text{XAD-7}}$) was used to calculate the amount of extractant immobilized on the EIR:

$$q_{IL} = \frac{M_{\text{XAD-7/Cyphos IL 101}} - M_{\text{XAD-7}}}{M_{\text{XAD-7/Cyphos IL 101}}} \quad (1)$$

The experimental procedure allowed the preparation of EIRs containing 106 mg extractant g^{-1} EIR up to 586 mg extractant g^{-1} EIR.

Sorption and Desorption Studies

Hg(II) solutions were prepared in HCl solutions of different concentrations (0.01–2*M*) with metal concentrations ranging between 10 and 250 mg Hg L^{-1}. The sorption experiments at equilibrium (effect of HCl concentration and IL loading on Hg(II) sorption efficiency, and sorption isotherms) were performed by mixing the resin with Hg(II) solutions for 48 h with a solid/liquid ratio (sorbent dosage) fixed to $m/V = 2$ g L^{-1} (m: mass of sorbent, V: volume of solution). The contact was operated on a reciprocal shaker (SEV, model INO 650 V-7, Mexico) with an agitation speed of 150 movements per minute at constant temperature. After resin separation the samples were analyzed by spectrophotometry (spectrophotometer Varian, Cary 50 Probe) using a procedure adapted from the dithizone method (wavelength $\lambda = 492$ nm).[42] The amount of metal adsorbed (q, mg Hg g^{-1}) was calculated by the mass balance equation: $q = V(C_0 - C_{eq})/m$, where C_0 and C_{eq} (mg Hg L^{-1}) are the initial and equilibrium Hg(II) concentrations, respectively.

Several sorption kinetic experiments were performed by contact under agitation of a fixed amount of EIR (IL loading: 106, 207, 401, or 586 mg extractant g^{-1}) with a fixed volume (m/V: 2 g L^{-1}) of 1*M* HCl solution a concentration of Hg(II) of 250 mg Hg(II) L^{-1}. Temperature was varied in the range 10–40°C. The agitation speed was set at 150 rpm (or alternatively to 250 rpm when investigating the effect of agitation speed). Detailed

experimental conditions are reported in the caption of the figures. Solution samples were withdrawn at preselected contact times; there were analyzed for Hg(II) content using the dithizone method.

For the study of Hg(II) desorption, an amount of 20 mg of EIR (extractant loading: 401 mg IL g^{-1}) was mixed with 10 mL of Hg(II) solution (1*M* HCl solution, initial metal concentration: 100 mg Hg(II) L^{-1}) for 24 h. The residual concentration measured by the dithizone method after resin separation served to determine the amount of metal bound to the resin. The metal-loaded resin was mixed for 48 h with 10 mL of a series of eluents: 6*M* HNO_3 or 1*M* thiourea in 1*M* HCl. After resin separation the metal concentration in the eluent was determined by the dithizone method to obtain the amount of Hg(II) desorbed from the resin. The amount of metal desorbed divided by the amount of metal bound to the EIR served for calculating the desorption yield (or efficiency). After metal desorption the EIR was rinsed three times with 10 mL of water for 8 h to remove the residual eluent. For the evaluation of sorption/desorption cycles, the same procedure was used for five cycles.

Though the release of IL from EIR was not quantified, previous studies[31] have shown that below a critical IL loading (close to 600–650 mg IL g^{-1} EIR) the IL remains stable in the porous structure of the EIR. Above this critical value water extraction during the sorption phase contributes to increase the volume occupied by the IL in the porous structure, leading, in a second step, to a partial release of the IL in the solution.

Modeling of Sorption Isotherms and Uptake Kinetics

Sorption isotherms represent the distribution of the solute at equilibrium between the solid phase (the sorbent) and the liquid phase (the solution). The plot of q versus C_{eq} can be modeled using a number of equations. The equations of Freundlich and Langmuir are the most commonly used. The Freundlich equation supposes an exponential trend while the Langmuir is characterized by an asymptotic shape. As the sorption capacity tended to an asymptotic value (experimental maximum sorption capacity) the isotherm will be preferentially described by the Langmuir equation rather than the Freundlich equation.

$$\text{Langmuir equation} : q = \frac{q_m b C_{eq}}{1 + b\ C_{eq}} \tag{2}$$

with q_m (mg metal g^{-1} or mmol metal g^{-1}), b (L mg^{-1} or L $mmol^{-1}$) are the constants of the Langmuir equation: the sorption capacity at saturation of the monolayer and the affinity coefficient, respectively. The parameters of the Langmuir equation were obtained using the plot of $C_{eq}/q = f(C_{eq})$.

The uptake kinetics can be controlled by a series of mechanisms including the proper chemical reaction rate (CR) but also by diffusion mechanisms [including resistance to bulk diffusion, to film diffusion (FD) and to intraparticle diffusion (PD)]. The identification of the controlling step is important for optimizing the process; this allows selecting best experimental conditions or optimizing the design of the sorbent (for limiting, e.g., resistance to PD). Actually, the modeling of uptake kinetics should take into account all these mechanisms (FD, PD, reaction rate, equilibrium distribution, etc.) at the expense of using complex numerical analysis systems.[43] Juang and Ju[44] discussed a series of simplified modeling systems derived from the homogeneous diffusion model (HDM) and the shrinking core model (SCM). The HDM involves counterdiffusion of exchangeable species in quasihomogeneous media, with a contribution from FD (HDM-FD) and/or particle diffusion (HDM-PD). Solute molecules and exchangeable species (immobilized on the resin) follow a similar diffusion mechanism (but in the opposite direction). In the case of the SCM, a sharp virtual boundary exists between the reacted shell of the particle and the unreacted core, and this boundary moves toward the center of the particle.[45,46] This model was developed with different systems depending on the controlling step: FD (SCM-FD), particle diffusion (SCM-PD), and CR (SCM-CR).[44] A number of mathematical equations have been developed to simulate these mechanisms, they are listed below:

Homogeneous Diffusion Model.

$$\text{FD} : F_1(X) = -\ln(1-X) = f(t) \tag{3}$$

$$\text{PD} : F_2(X) = -\ln\left(1-X^2\right) = f(t) \tag{4}$$

Shrinking Core Model.

$$\text{FD} : G_1(X) = X = g\left(\int_0^t C(t)\ dt\right) \tag{5}$$

$$\text{PD} : G_2(X) = 3-3(1-X)^{2/3} - 2X = g\left(\int_0^t C(t)\ dt\right) \tag{6}$$

$$\text{CR} : G_3(X) = 1-(1-X)^{1/3} = g\left(\int_0^t C(t)\ dt\right) \tag{7}$$

Where X is the fractional approach to equilibrium (i.e., $q(t)/q_{eq}$), the amount adsorbed at time t divided by the amount of metal adsorbed at equilibrium. Plotting F_i and G_i functions versus time and the integral term (respectively) determined the most appropriate mechanism for describing the controlling step. The curve giving a straight line (good correlation measured by the correlation coefficient) is the predominant limiting step.

The kinetics have been modeled using four conventional models: (a) the pseudofirst order rate equation (the Lagergren equation), (b) the pseudosecond order rate equation, (c) the resistance to FD, and (d) the simplified approach of PD (the Crank equation).

The reaction rate equations were initially designed for describing CRs in homogeneous systems. However, they are frequently used for the description of sorption kinetics; although they underestimate the contribution of diffusion mechanisms.

Pseudo*first* Order Rate Equation.[47]

$$\frac{dq(t)}{dt} = k_1(q_{eq} - q(t)) \tag{8}$$

and after integration:

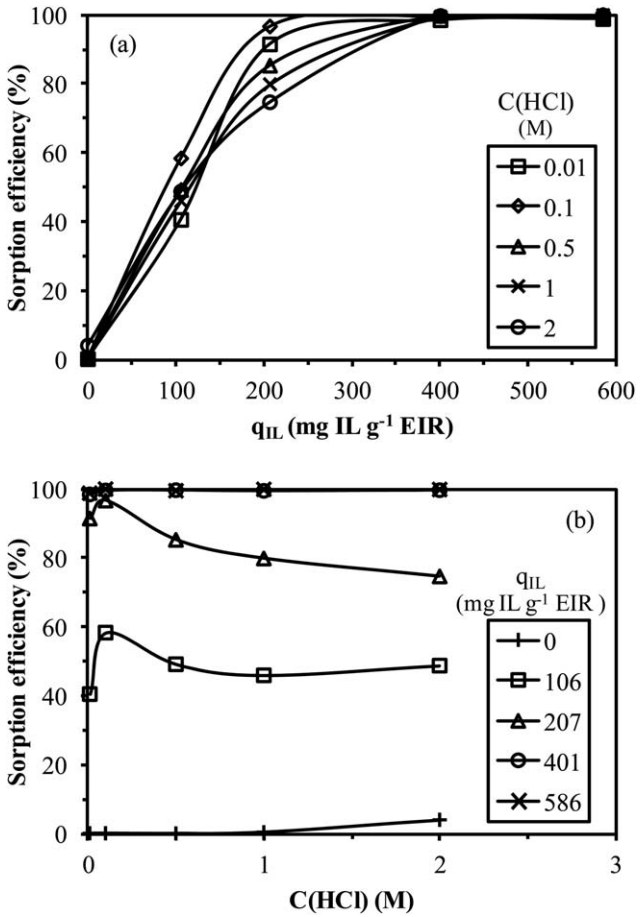

Figure 1. Effect of HCl concentration and IL loading on Hg(II) sorption efficiency using Amberlite XAD-7 impregnated with Cyphos IL 101 (C_0: 100 mg Hg L^{-1}; m/V: 2 g L^{-1}; T: 20°C).

$$\ln\left(1-\frac{q(t)}{q_{eq}}\right)=-k_1 t \tag{9}$$

where q_{eq} (mg g^{-1}) is the sorption capacity at equilibrium (parameter of the model, determined by data analysis to be compared to the experimental value as a validation criterion), k_1 (min^{-1}) is the pseudofirst order rate constant.

Pseudosecond Order Rate Equation.[48]

$$\frac{dq(t)}{dt}=k_2(q_{eq}-q(t))^2 \tag{10}$$

and after integration:

$$q(t)=\frac{q_{eq}^2 k_2 t}{1+q_{eq} k_2 t} \tag{11}$$

where q_{eq} (mg g^{-1}) is the sorption capacity at equilibrium (parameter of the model, determined by data analysis to be compared to the experimental value as a validation criterion), k_2 (g mg^{-1} min^{-1}) is the pseudosecond order rate constant.

The parameters of the models [eqs. (9) and (11)] were determined using the nonlinear regression analysis of experimental data with the Mathematica® software.

Apart of these models that take into account only the reaction, diffusion mechanisms can be also involved in the control of uptake kinetics: (a) resistance to external diffusion (through the film surrounding the particles) and (b) the resistance to PD. The resistance to bulk diffusion is generally neglected as this limiting step can be easily overcome providing sufficient agitation to the reactor. The resistance to FD is generally the predominant step in the initial phase of the sorption process while the resistance to PD plays a greater role in the later phase.

The PD coefficient (D_e, effective diffusivity, m^2 min^{-1}) has been determined using the Crank's equation (RIDE, resistance to intraparticle diffusion equation),[49] assuming the solid to be initially free of metal, and external diffusion resistance not being the limiting step at long contact time:

$$\frac{q(t)}{q_{eq}} = 1-\sum_{n=1}^{\infty}\frac{6\alpha(\alpha+1)\exp\left(\frac{-D_e q_n^2 t}{r^2}\right)}{9+9\alpha+q_n^2\alpha^2} \tag{12}$$

q_n nonzero roots of the equation:

$$\tan q_n = \frac{3\ q_n}{3+\alpha\ q_n^2} \tag{13}$$

$$\text{with } \frac{q}{VC_o} = \frac{1}{1+\alpha} \text{ and } r \text{ being the radius of the particle} \tag{14}$$

The eqs. (12–14) were used with the Mathematica® package for the determination of the PD coefficient.

RESULTS AND DISCUSSION

Effect of HCl Concentration and IL Loading on Hg(II) Sorption Efficiency

Figure 1 shows the cross effects of IL loading and HCl concentration on sorption efficiency. As expected when increasing the IL loading the sorption increases regardless of HCl concentration [Figure 1(a)]. The sorption linearly increases with IL loading till 200 mg IL g^{-1} EIR, under selected experimental conditions. Above, the excess of IL (compared to metal amount) leads to the complete recovery of mercury and the effect of HCl concentration cannot be detected. For 207 mg IL g^{-1} EIR loading, the sorption progressively decreased when increasing HCl concentration. At pH 1–2, the mercury is almost completely recovered (higher than 90%), while in 2*M* HCl the sorption efficiency falls under 75%. When the concentration of acid increases the IL amount required for complete Hg(II) recovery increases. This is probably due to (a) the coextraction of HCl (which limits the availability of phosphonium cations) and (b) the change in the speciation of Hg(II) in solution.

The second panel of the figure [Figure 1(b)] shows distinct trends on the effect of HCl concentration for low IL loadings. In the absence of IL, Amberlite XAD-7 does not bind Hg(II), at least in solutions containing less than 2*M* HCl. In 2*M* HCl solutions, the sorption slightly increases, though the sorption efficiency remained below 5% under selected experimental conditions. This phenomenon was observed in the case of Cd(II) recovery from HCl solutions using the same EIR.[31] The contribution of Amberlite XAD-7 on direct binding of Au(III) in concentrated HCl solutions was even more important.[33] This can be explained by different mechanisms; the most probable being the extraction of HCl by the resin through interactions

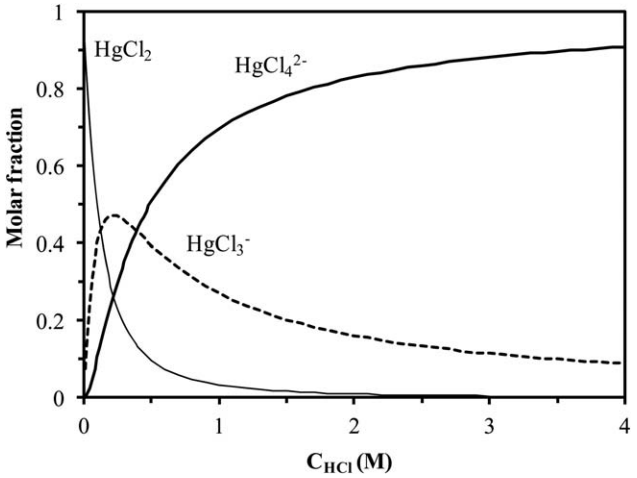

Figure 2. Hg(II) speciation in function of HCl concentration.

with oxygen atoms on the polyacrylic matrix (═O ··H^+Cl^-), followed by the exchange of chloride anions with cadmium chloroanions (═O · ·$H^+CdCl_4^{2-}$, or ═O · ·$H^+CdCl_3^-$). At high IL loading, the metal is completely removed from the solution, regardless of HCl concentration. Even in the less favorable conditions (i.e., high HCl concentration) the excess of IL maintains the possibility to remove all the metal. In the intermediary range of IL loading (i.e., at 106 or 207 mg IL g^{-1} EIR), the sorption efficiency profiles are more interesting. They show that the speciation has a significant impact on sorption efficiency. Indeed, when the HCl concentration increases from 0.01 to 0.1*M* the sorption efficiency increases, this is consistent with the formation of chloroanionic species: $HgCl_3^-$ and to a lesser extent $HgCl_4^{2-}$ (Figure 2). The constants of the Hg(II) complexation were taken from Puigdomenech.[50] When the concentration of HCl increases above 0.1*M* (and up to 1*M*) the sorption efficiency tends to decrease. This diminution can probably be explained by the double effect of (a) the HCl competition and (b) the predominance of $HgCl_4^{2-}$ versus $HgCl_3^-$ (at higher charge, higher affinity but lower sorption capacity). At 2*M* HCl concentration the sorption efficiency tends to stabilize. The shape of the curves at intermediary IL loading (which allows measuring the limiting effects) suggests that the EIR has a preference for $HgCl_3^-$ or that the binding affinity of Hg(II) chloroanionic species for the EIR is not so strong as for some other metal ions [such as Au(III),[33] Zn(II),[30] and Pt(IV)[34]] that were not affected so much by HCl concentration (which involves competition for binding to phosphonium cation).

The distribution coefficient (D, L kg^{-1}) is calculated as the ratio of the sorption capacity to the residual concentration at equilibrium ($D = q/C_{eq}$). Figure 3 shows the influence of IL loading and HCl concentration on the distribution coefficient (log–log plot). The distribution coefficient increases with IL loading; a significant dispersion in the distribution coefficient is observed at high IL loading. Based on the results showed on Figure 1, at high IL loading (i.e., 586 mg IL g^{-1} EIR), the excess of IL leads to almost complete recovery of the metal. As a consequence some analytical discrepancies can be associated to the determination of residual concentration, which induce data dispersion. On another side, a partial precipitation was observed at high IL loading in highly concentrated HCl solutions: the nature of the precipitate was not clearly identified (though it contained mercury). The precipitate only occurred in the simultaneous presence of IL and Hg(II). Regardless of the nature of this precipitate this is sufficient for introducing some discrepancies in the determination of the distribution coefficients at high IL loading. The logarithm of the distribution coefficient varies linearly with the logarithm of IL loading, regardless of the concentration of HCl. The slope of the curves is close to 4. This value is significantly different to the value expected (i.e., 2 or 1) from the hypothesis of a binding of Hg(II) through the interaction of chloroanionic species ($HgCl_4^{2-}$ and $HgCl_3^-$, respectively) with phosphonium cation. These discrepancies may be explained by the difficulty to accurately determine the amount of IL really free in the EIR (which is the sole quantity of IL to be taken into account in the slope analysis method). Indeed, a number of different parameters may affect the distribution of the IL, and they are not systematically quantifiable: amount of mercury bound to the IL, stoichiometry of the complex, coexistence of different species, interactions of the support with mercury, coextraction of HCl and water by the IL, and so forth. Conversely, Figure 3(b) shows that the distribution coefficient hardly varied with the concentration of HCl. This result tends to minimize the impact of HCl concentration on the distribution of mercury between the liquid and the solid phases at equilibrium. This means that metal speciation will have a weak

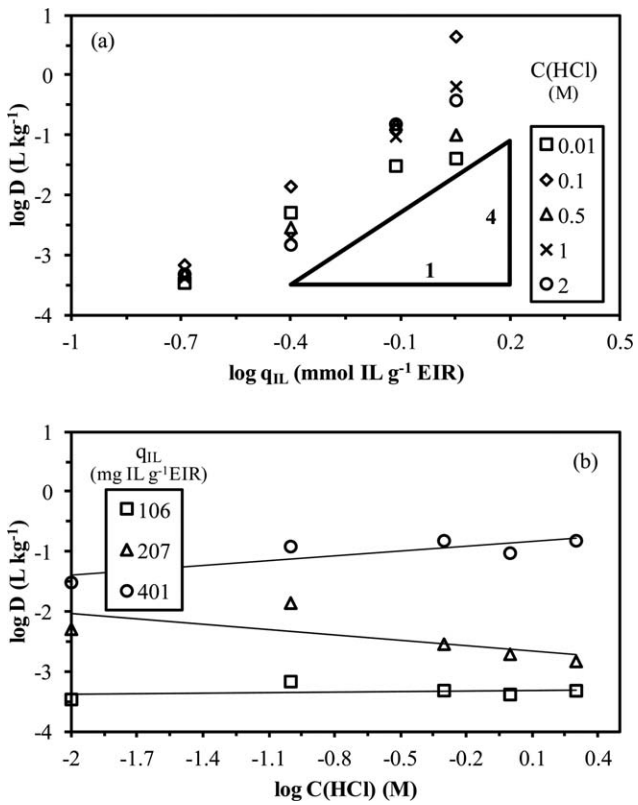

Figure 3. Effect of HCl concentration and IL loading on Hg(II) distribution coefficient D using Amberlite XAD-7 impregnated with Cyphos IL 101 (C_0: 100 mg Hg L^{-1}; m/V: 2 g L^{-1}; T: 20°C).

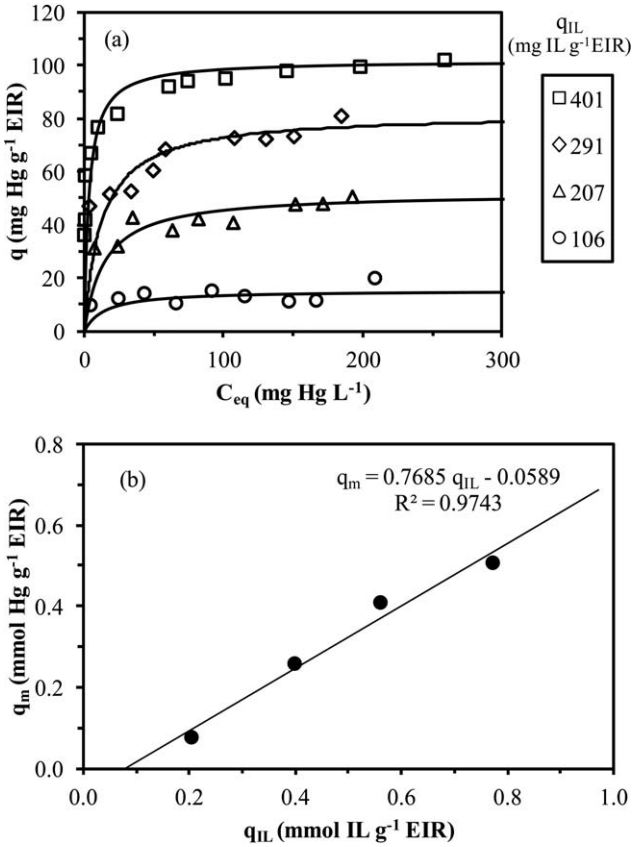

Figure 4. (a) Hg(II) sorption isotherms for different IL loadings using Amberlite XAD-7 impregnated with Cyphos IL101 [C(HCl): 1*M*] and (b) correlation between the maximum sorption capacity (q_m) of the EIR and the IL loading (q_{IL}).

impact on metal recovery, at least compared to the effect of IL loading. The data obtained with the IL loading of 586 mg IL g^{-1} were not taken into account because of the wide dispersion of data due to precipitation phenomena.

Effect of IL Loading on Hg(II) Sorption Isotherm

The sorption isotherms have been determined in 1*M* HCl solutions for increasing IL loadings [Figure 4(a)]. All the curves show a similar shape: (a) a first initial steep slope, followed by (b) a saturation plateau reached at low residual concentration. This means that the sorption isotherm can be considered as a quasi irreversible sorption isotherm. The saturation plateau (which corresponds to an asymptotic shape) indicates that the system will be better described by the Langmuir equation than by the Freundlich equation (exponential profile). The isotherm for the EIR with the highest IL loading (586 mg IL g^{-1} EIR) was excluded due to a partial precipitation of mercury (under an unidentified form) for the highest metal concentrations. Moreover, in this case, high values dispersion was observed due to a very slow sorption speed of EIR with high IL loading (see uptake kinetics section). Table II reports the parameters of the Langmuir equation for the different IL loadings. The molar ratio between the metal and the IL varies between 0.38 and 0.73 mol mol^{-1}. The affinity coefficient (b) is also increasing with IL loading. The coefficient $q_m \times b$ (L g^{-1}), analogous to the distribution coefficient, is also increasing with IL loading (increasing from 1.06 to 30.45 L g^{-1} when the IL loading increases from 106 to 401 mg IL g^{-1} EIR). Figure 4(b) shows the correlation of the maximum sorption capacity with the IL loading (in the concentration range: 106–401 mg IL g^{-1} EIR). The slope of the curve is equal to 0.77: this value is intermediary between the theoretical Hg/IL molar ratios 1 : 1 (for the $R_3R'P^+ \cdot HgCl_3^-$ complex) and 2 : 1 (for the $(R_3R'P^+)_2 \cdot HgCl_4^{2-}$ complex). This means that the EIR is probably able to sorb mercury through the binding of both $HgCl_3^-$ and $HgCl_4^{2-}$, according to the next reactions, considering $HgCl_4^{2-}$ as the predominant Hg(II) species in solution (C(HCl) > 0.4*M*):

$$R_3R'P^+ \cdot Cl^- + HgCl_4^{2-} \leftrightarrow R_3R'P^+ \cdot HgCl_3^- + 2Cl^- \quad (15a)$$

$$2R_3R'P^+ \cdot Cl^- + HgCl_4^{2-} \leftrightarrow (R_3R'P^+)_2 \cdot HgCl_4^{2-} + 2Cl^- \quad (15b)$$

It is noteworthy that the ordinate intercept [Figure 4(b)] is negative (i.e., −0.059). This means that a fraction of the IL (about 0.077 mmol IL g^{-1}; i.e., close to 40 mg IL g^{-1}) does not contribute to metal sorption. It is suspected that this fraction is involved in interactions with the support. A similar phenomenon was observed in the case of Cd(II) sorption using the same type of EIR.[31]

Hg(II) Uptake Kinetics

The uptake kinetics can be controlled by a series of mechanisms including the proper CR but also by diffusion mechanisms.[43–49] The identification of the controlling step is important for optimizing the process.

Effect of Agitation Speed on Hg(II) Uptake Kinetics. The uptake kinetics have been studied using the SCM and the HDM associated with resistance to either FD, PD, or CR (see Supporting Information). The plots clearly show that in all cases the linearization of experimental data corresponds to systems governed by the resistance to PD (with either SCM or HDM).

The agitation speed is a critical parameter for the evaluation of the contribution of resistance to FD on the overall uptake kinetics. Generally, at low agitation regime the thickness of the film surrounding the sorbent particles increases; this, in turn, increases the resistance to external diffusion. The kinetic profiles were compared at two different agitation speeds (i.e., 150 and

Table II. Parameters of the Langmuir Equation for the Sorption of Hg(II) Using Amberlite XAD-7 Impregnated with Different Amounts of Cyphos IL101 (*T*: 20°C; *v*: 150 rpm)

q_{IL} (mg IL g^{-1} EIR)	q_m (mg Hg g^{-1} EIR)	b (L mg^{-1})	$q_m \times b$ (L g^{-1})	q_m/q_{IL} (mol mol^{-1})
106	15.3	0.069	1.06	0.38
207	51.7	0.069	3.57	0.65
291	81.9	0.080	6.52	0.73
401	101.5	0.300	30.45	0.66

q_m: sorption capacity at saturation of the monolayer; b: affinity coefficient.

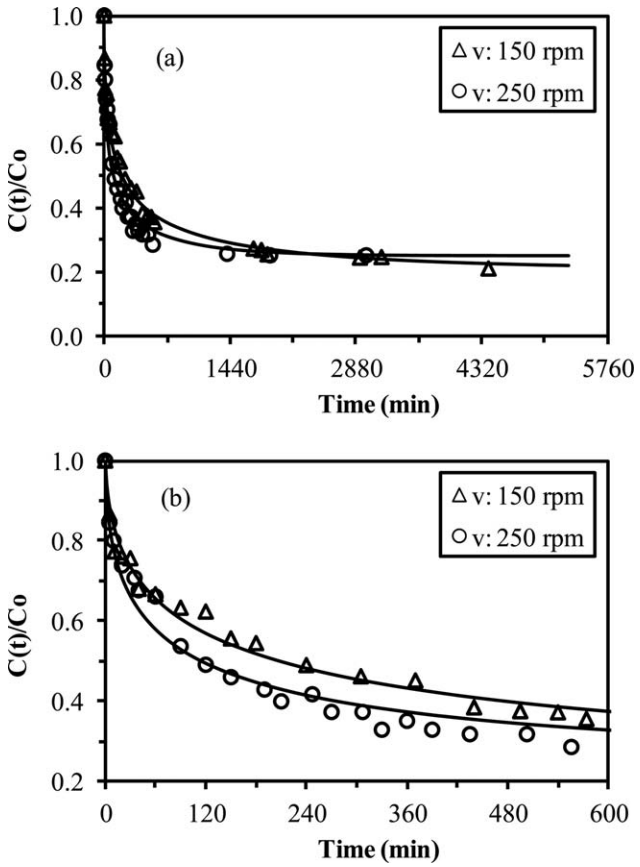

Figure 5. Influence of agitation speed on Hg(II) recovery from 1*M* HCl solutions using Amberlite XAD-7 impregnated with Cyphos IL 101: (a) complete kinetics and (b) initial section of the kinetics (solid lines: modeling of uptake kinetics with the RIDE).

250 rpm, Figure 5). The general view [Figure 5(a)] shows that the profiles overlap and the residual concentrations tend to the same equilibrium value. This is consistent with the conclusions derived from the plots of SCM and HDM (see Supporting Information). This behavior was also observed in the sorption of other metals using the same material[30–34]: the agitation speed hardly influences the sorption kinetics using Amberlite XAD-7 impregnated with Cyphos IL 101. A slight variation appears at the beginning of the contact phase [Figure 5(b)]: the curve obtained at the agitation speed of 250 rpm is slightly more favorable than that obtained at 150 rpm. However, the differences are not very marked indicating that the resistance to FD is probably not the limiting step in the mass transfer. Table III reports the values of the PD coefficient (D_e) determined using the Crank's equation (RIDE). D_e slightly increases with the agitation speed, in the range 1.98–6.12 $\times$ 10^{-12} m^2 min^{-1}. These values are in the lower range compared with those obtained with Au(III) (i.e., 1.8–16.6 $\times$ 10^{-11} m^2 min^{-1}),[33] Zn(II) (i.e., 1.2–5.9 $\times$ 10^{-11} m^2 min^{-1}),[30] Pd(II) (i.e., 2.0–20.0 $\times$ 10^{-11} m^2 min^{-1})[32], and Cd(II) (i.e., 0.2–9.9 $\times$ 10^{-10} m^2 min^{-1}).[31] The agitation speed has a limited impact on the k_2 coefficient of pseudosecond order rate equation, which decreases from 1.85 $\times$ 10^{-4} to 1.22 $\times$ 10^{-4} g mg^{-1} min^{-1} when the agitation speed decreased from 250 to 150 rpm. These values are consistent

Table III. Uptake Kinetics—RIDE) – —Intraparticle Diffusion Coefficient (D_e)

q_{IL} (mg IL g^{-1} EIR)	v (rpm)	T (°C)	$D_e \times 10^{12}$ (m^2 min^{-1})	SSR
401	250	20	6.12	0.047
106	150	20	265.1	0.069
207	150	20	37.88	0.049
401	150	20	1.98	0.021
586	150	20	0.064	0.074
401	150	10	2.56	0.112
401	150	40	14.7	0.081

SSR: Sum of square of residuals.

with those obtained in the binding of Pt(IV) (i.e., 0.38–5.26 $\times$ 10^{-4} g mg^{-1} min^{-1}),[39] Pd(II) (i.e., 0.65–18.5 $\times$ 10^{-4} g mg^{-1} min^{-1}),[38] Cd(II) (i.e., 0.63–8.01 $\times$ 10^{-4} g mg^{-1} min^{-1})[40], and Hg(II) (i.e., 1.6–9.2 $\times$ 10^{-4} g mg^{-1} min^{-1})[37] using Cyphos immobilized in alginate capsules.

Effect of IL Loading on Hg(II) Uptake Kinetics. The load of IL in the EIR may strongly impact the uptake kinetics. Arias et al.[31] have shown that when increasing the amount of IL immobilized in Amberlite XAD-7 the uptake kinetics was slowed down. Two sets of experiments were performed: (a) changing the amount of sorbent but maintaining constant the total amount of extractant and (b) changing the amount of sorbent but maintaining constant the equilibrium concentration. In the two series, the profiles corresponding to the lower IL loading reached faster the equilibrium than the other EIRs. They suggested that the progressive filling of the porous network contribute to reducing the mass transfer of the solute: the diffusion in the IL phase is supposed to occur slower than in the aqueous phase. These results were correlated to the specific surface area of the resin that progressively decreased with increasing IL loading. The micropores were saturated before the mesopores and macropores were progressively filled, which, in turn, limited the PD of metal ions. The present results are consistent with these hypotheses: the contact time required for reaching the equilibrium significantly increases with IL loading. Tables (III–V) and Figure 6(c) show that all the kinetic parameters (PD, k_1 coefficient of pseudofirst order rate equation, and k_2 coefficient of pseudosecond order rate equation) are strongly reduced when the IL loading increases. This is consistent with the decrease of the PD coefficient with the increase of IL loading for Cd(II) sorption,[31] Au(III) sorption,[33] and Pd(II)[32] using the same EIR. In the case of α-phenylglycine extraction with an extractant-impregnated macroporous resin, Ruiz et al.[51] observed an increase of the PD coefficient with extractant loading. In the case of Bi(III) recovery using a D2EHPA-impregnated resin (Amberlite XAD-1180), Belkhouche and Didi[52] observed that the sorption kinetics is faster at low extractant content of the resin. Benamor et al.[53] discussed the effect of extractant loading on Amberlite XAD-7 impregnated with D2EHPA for the sorption of Cd(II). They observed that at pH 4 the loading of the resin had a very limited effect on

Table IV. Uptake Kinetics—Constants of the Pseudofirst Order Rate Equation

q_{IL} (mg IL g^{-1} EIR)	v (rpm)	T (°C)	$q_{m,exp}$ (mg Hg g^{-1} EIR)	$q_{m,mod}$ (mg Hg g^{-1} EIR)	k_1 10^2 (min^{-1})	SSR
401	250	20	100.0	90.8	1.31	58.1
106	150	20	30.7	30.3	11.13	2.52
207	150	20	50.7	47.2	3.14	28.9
401	150	20	105.0	91.8	0.77	127.5
586	150	20	125.5	99.8	0.29	92.5
401	150	10	99.9	95.0	0.52	97.0
401	150	40	93.3	91.2	2.18	16.8

SSR: Sum of square of residuals.

kinetic profiles contrary to pH 3 for which the sorption kinetics was faster at low extractant load.

Effect of Temperature on Hg(II) Uptake Kinetics. The temperature slightly influences the kinetic profiles, especially in the initial section of the curve (Figure 7). Although the curves almost overlap between 10 and 20°C, at 40°C the uptake kinetics was enhanced. This is confirmed by the comparison the kinetic coefficients: k_1, k_2, and D_e significantly raised when the temperature was increased from 10–20°C to 40°C (Tables III–V). The presence of water or organic solvent strongly reduces the viscosity and the density of IL.[54] The IL is coextracting HCl and water in acidic solutions: this may contribute to decrease the viscosity of the IL immobilized in the porous network, which, in turn, may reduce the resistance to PD. This beneficial effect of water on the viscosity of IL is reinforced by the temperature (Cytec Technical Data). The improvement of mass transfer properties by increasing the temperature confirms the contribution of the resistance to PD on the control of uptake kinetics: decreasing the viscosity of the IL phase in the porous network improves uptake kinetics.

Hg(II) Desorption from Loaded EIR and EIR Recycling

The desorption of the metal from loaded EIR and the recycling of the sorbent is a key criterion for the transfer of the metal recovery technology to larger scale. To evaluate the potential of these materials a series of five sorption/desorption cycles was performed using (a) 1*M* thiourea in 1*M* HCl solution and (b) 6*M* HNO_3. Preliminary tests showed that molar solutions of thiourea and HCl allowed efficient desorption of mercury: the high affinity of thiourea for binding mercury can explain the choice of this eluent; the presence of HCl reinforce its efficiency. The association of thiourea with HCl has been frequently cited for the desorption of precious metals [including Pd(II), Pt(IV), or Au(III) from loaded resins and EIRs][33,36,38,39,55] and Hg(II).[6,9,16] Figure 8 confirms the highly efficiency of acidic thiourea solutions for the desorption of mercury from loaded EIR: though the desorption efficiency progressively decreases with the number of cycles, at the fifth cycle Hg(II) removal reached 90%. On the other side, under selected experimental conditions, the total recovery of mercury was achieved along the five cycles. In the case of nitric acid solution, the sorption/desorption performance was even better: sorption level was maintained at 100% for the five cycles while the desorption began to slightly decrease only at the fifth cycle. Nitric acid sounds more efficient and appropriate for the desorption of mercury loaded on the EIR: easier, less expensive, the eluate is less difficult to treat; in addition the resin can be recycled more efficiently. The nitric acid solution contributes to displace the speciation of mercury chloroanionic species toward the formation of mercury cations that cannot bind to protonated phosphonium cations: mercury can then desorb (contrary to the action of thiourea that complex mercury). The resin can be efficiently used for a minimum number of five sorption/desorption cycles. These results confirm that the EIR can be used for the recovery of Hg(II) from acidic

Table V. Uptake Kinetics—Constants of the Pseudosecond Order Rate Equation

q_{IL} (mg IL g^{-1} EIR)	v (rpm)	T (°C)	$q_{m,exp}$ (mg Hg g^{-1} EIR)	$q_{m,mod}$ (mg Hg g^{-1} EIR)	$k_2 \times 10^4$ (g mg^{-1} min^{-1})	SSR
401	250	20	100.0	100.9	1.85	21.0
106	150	20	30.7	31.6	68.1	1.65
207	150	20	50.7	50.5	9.73	13.2
401	150	20	105.0	99.1	1.22	55.6
586	150	20	125.5	117.4	0.28	56.5
401	150	10	99.9	104.7	0.70	60.5
401	150	40	93.3	98.0	3.31	9.66

SSR: sum of square of residuals.

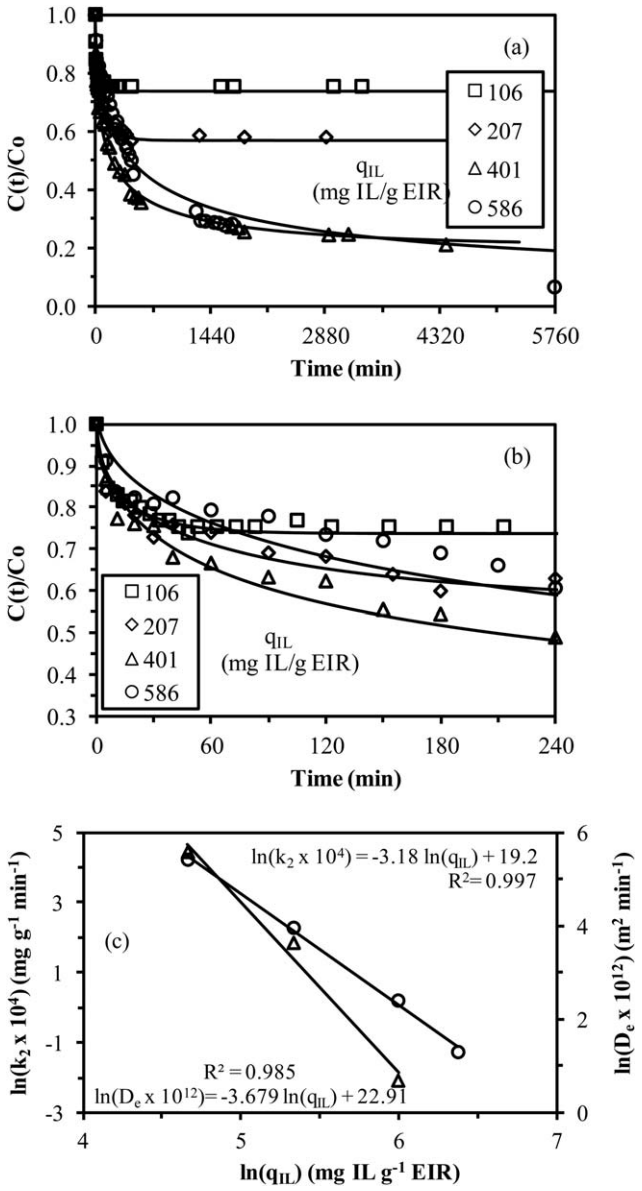

Figure 6. Influence of IL loading on Hg(II) recovery from 1*M* HCl solutions using Amberlite XAD-7 impregnated with Cyphos IL 101: (a) complete kinetics, (b) initial section of the kinetics, (c) correlation between pseudosecond order rate parameter (and PD coefficient) and IL loading (solid lines: modeling of uptake kinetics with the RIDE).

solutions and that the sorbent can be recycled making possible the use of these materials for larger scale application.

CONCLUSIONS

The impregnation of Amberlite XAD-7 with Cyphos IL 101 (tetraalkylphosphonium chloride) allows preparing EIRs that are very efficient for the recovery of mercury from HCl solutions. The sorption efficiency depends on the concentration of HCl and the IL loading. When increasing HCl concentration it is necessary increasing IL loading for maintaining total metal recovery (under selected experimental conditions). The cross-impact of these parameters points out the importance of metal speciation on sorption efficiency. Metal binding occurs through the ion exchange between chloroanionic mercury species ($HgCl_3^-$ and $HgCl_4^{2-}$) and $R_3R'P^+ \cdot Cl^-$. Sorption isotherms are described by the Langmuir equation: the maximum sorption capacity linearly increases with IL loading up to 0.5 mmol Hg g^{-1} (i.e., 100 mg Hg L^{-1}) in 1*M* HCl solutions. A fraction of the IL immobilized on the resin (about 0.077 mmol IL g^{-1}; 40 mg IL g^{-1}) seems to be inactive being involved in strong interaction with the support. The limited impact of agitation speed tends to indicate that the resistance to FD is not rate limiting, contrary to the resistance to PD that plays a major role on the control of uptake kinetics. The temperature has a limited impact while the IL loading significantly influences the sorption kinetics, especially at high IL loading (above 500 mg IL g^{-1}). The complete filling of the internal porosity with the IL contributes to limiting mass transfer in the EIR (as shown by the dramatic decrease of the PD coefficient from 2.6×10^{-10} m^2 min^{-1} at IL: 106 mg IL g^{-1} to 6.0×10^{-14} m^2 min^{-1} at IL: 586 mg IL g^{-1}). An intermediary IL loading (i.e., 300–400 mg IL g^{-1}) sounds to be preferable for optimizing both accessibility and availability of IL for mercury. Despite the efficiency of thiourea (in HCl solution) for recovering mercury from loaded EIR, nitric acid sounds to be more efficient for the combined metal recovery and EIR recycling. The two eluents allow maintaining

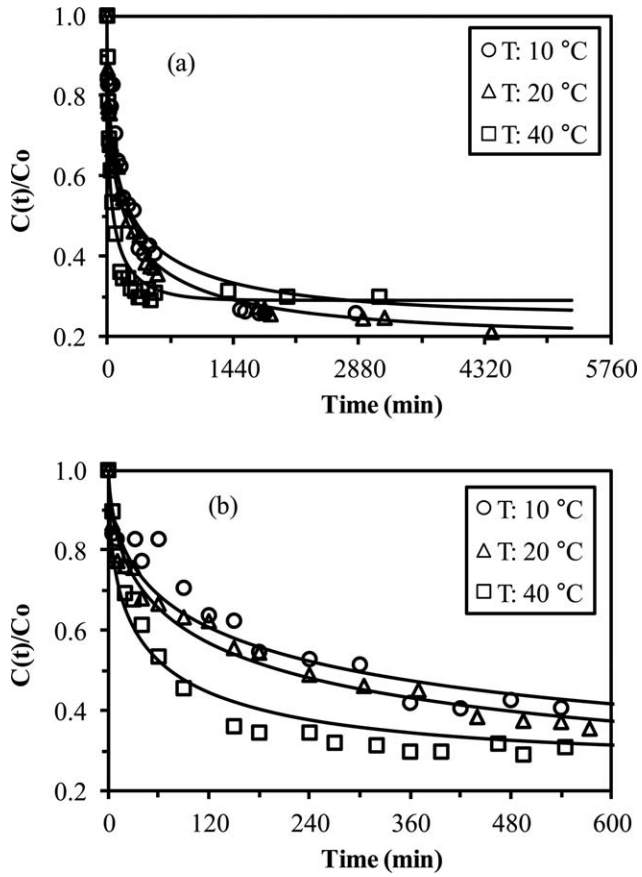

Figure 7. Effect of temperature on Hg(II) recovery from 1*M* HCl solutions using Amberlite XAD-7 impregnated with Cyphos IL 101: (a) complete kinetics and (b) initial section of the kinetics (solid lines: modeling of uptake kinetics with the RIDE).

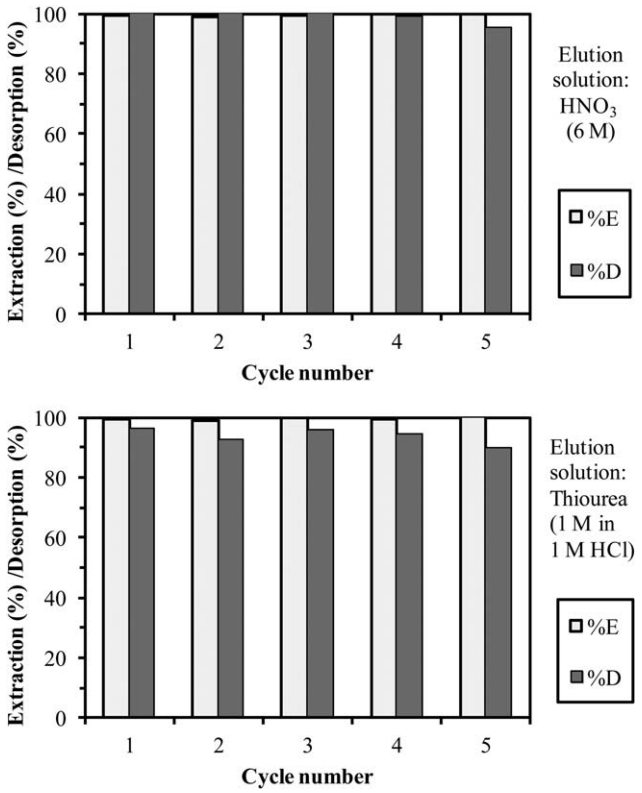

Figure 8. Sorption and desorption cycles for Hg(II) using Amberlite XAD-7 impregnated with Cyphos IL101 (experimental conditions: adsorption: C_0: 100 mg Hg L^{-1}; m/V: 2 g L^{-1}; T: 20°C; q_{IL}: 401 mg IL g^{-1} EIR; C(HCl): 1*M*; desorption: m/V: 2 g L^{-1}).

a good sorption of mercury over fives cycles; however, the desorption appears to be more complete with nitric acid than with thiourea.

ACKNOWLEDGMENTS

Authors thank the University of Guanajuato (CIAI 2013, 279/13) for financial support. Cytec (Canada) is acknowledged for the gift of Cyphos IL 101 sample.

REFERENCES

1. Fulbright, H. H.; Leaphart, M.; VanBrunt, V. *Sep. Sci. Technol.* **1997**, *32*, 373.
2. Wajima, T.; Sugawara, K. *Fuel Process. Technol.* **2011**, *92*, 1322.
3. Shawky, H. A.; El-Aassar, A. H. M.; Abo-Zeid, D. E. *J. Appl. Polym. Sci.* **2012**, *125*, E93.
4. Cataldo, S.; Gianguzza, A.; Pettignano, A.; Villaescusa, I. *React. Funct. Polym.* **2013**, *73*, 207.
5. Svecova, L.; Spanelova, M.; Kubal, M.; Guibal, E. *Sep. Purif. Technol.* **2006**, *52*, 142.
6. Gavilan, K. C.; Pestov, A. V.; Garcia, H. M.; Yatluk, Y.; Roussy, J.; Guibal, E. *J. Hazard. Mater.* **2009**, *165*, 415.
7. Lloyd-Jones, P. J.; Rangel-Mendez, J. R.; Streat, M. *Process. Saf. Environ. Protect.* **2004**, *82*, 301.
8. Atia, A. A.; Donia, A. M.; El-Nomany, H. H. *J. Disper. Sci. Technol.* **2009**, *30*, 451.
9. Ma, X.; Li, Y.; Ye, Z.; Yang, L.; Zhou, L.; Wang, L. *J. Hazard. Mater.* **2011**, *185*, 1348.
10. Sonmez, H. B.; Senkal, B. F.; Bicak, N. *J. Appl. Polym. Sci.* **2003**, *87*, 1316.
11. Yavuz, E.; Barim, G.; Senkal, B. F. *J. Appl. Polym. Sci.* **2009**, *114*, 1879.
12. Takagai, Y.; Shibata, A.; Kiyokawa, S.; Takase, T. *J. Colloid Interface Sci.* **2011**, *353*, 593.
13. Huebra, M.; Elizalde, M. P.; Almela, A. *Hydrometallurgy* **2003**, *68*, 33.
14. Rice, N. M.; Smith, M. R. *J. Appl. Chem. Biotechnol.* **1975**, *25*, 379.
15. Carreón, J.; Saucedo, I.; Navarro, R.; Maldonado, M.; Guerra, R.; Guibal, E. *Membr. Water Treat.* **2010**, *1*, 231.
16. Fontas, C.; Hidalgo, M.; Salvado, V.; Antico, E. *Anal. Chim. Acta* **2005**, *547*, 255.
17. Genc, O.; Arpa, C.; Bayramoglu, G.; Arica, M. Y.; Bektas, S. *Hydrometallurgy* **2002**, *67*, 53.
18. Gupta, B.; Ismail, Z. B. *Compos. Interfaces* **2006**, *13*, 487.
19. Liu, J. S.; Chen, H.; Guo, Z. L.; Hu, Y. C. *J. Appl. Polym. Sci.* **2006**, *100*, 253.
20. Zhu, L.; Liu, Y.; Chen, J.; Liu, W. *J. Appl. Polym. Sci.* **2011**, *120*, 3284.
21. Fischer, L.; Falta, T.; Koellensperger, G.; Stojanovic, A.; Kogelnig, D.; Galanski, M.; Krachler, R.; Keppler, B. K.; Hann, S. *Water Res.* **2011**, *45*, 4601.
22. Cieszynska, A.; Wisniewski, M. *Sep. Purif. Technol.* **2011**, *80*, 385.
23. Cieszynska, A.; Wisniewski, M. *Sep. Purif. Technol.* **2010**, *73*, 202.
24. Regel-Rosocka, M.; Wisniewski, M. *Hydrometallurgy* **2011**, *110*, 85.
25. Stojanovic, A.; Kogelnig, D.; Fischer, L.; Hann, S.; Galanski, M.; Groessl, M.; Krachler, R.; Keppler, B. K. *Aust. J. Chem.* **2010**, *63*, 511.
26. Kogelnig, D.; Stojanovic, A.; Jirsa, F.; Körner, W.; Krachler, R.; Keppler, B. K. *Sep. Purif. Technol.* **2010**, *72*, 56.
27. Liu, Y.; Guo, L.; Zhu, L.; Sun, X.; Chen, J. *Chem. Eng. J.* **2010**, *158*, 108.
28. Van den Berg, C.; Roelands, M.; Bussmann, P.; Goetheer, E.; Verdoes, D.; Van der Wielen, L. *Ind. Eng. Chem. Res.* **2008**, *47*, 10071.
29. Myasoedova, G. V.; Zakharchenko, E. A.; Molochnikova, N. P.; Myasoedov, B. F. *Radiochemistry* **2008**, *50*, 482.
30. Gallardo, V.; Navarro, R.; Saucedo, I.; Avila, M.; Guibal, E. *Sep. Sci. Technol.* **2008**, *43*, 2434.
31. Arias, A.; Navarro, R.; Saucedo, I.; Gallardo, V.; Martinez, M.; Guibal, E. *React. Funct. Polym.* **2011**, *71*, 1059.
32. Navarro, R.; Saucedo, I.; Gonzalez, C.; Guibal, E. *Chem. Eng. J.* **2012**, *−185186*, 226.
33. Navarro, R.; Saucedo, I.; Lira, M. A.; Guibal, E. *Sep. Sci. Technol.* **2010**, *45*, 1950.

34. Navarro, R.; Garcia, E.; Saucedo, I.; Guibal, E. *Sep. Sci. Technol.* **2012**, *47*, 2199.
35. Campos, K.; Domingo, R.; Vincent, T.; Ruiz, M.; Sastre, A. M.; Guibal, E. *Water Res.* **2008**, *42*, 4019.
36. Campos, K.; Vincent, T.; Bunio, P.; Trochimczuk, A.; Guibal, E. *Solvent Extr. Ion Exch.* **2008**, *26*, 570.
37. Guibal, E.; Gavilan, K. C.; Bunio, P.; Vincent, T.; Trochimczuk, A. *Sep. Sci. Technol.* **2008**, *43*, 2406.
38. Vincent, T.; Parodi, A.; Guibal, E. *React. Funct. Polym.* **2008**, *68*, 1159.
39. Vincent, T.; Parodi, A.; Guibal, E. *Sep. Purif. Technol.* **2008**, *62*, 470.
40. Guibal, E.; Figuerola Piñol, A.; Ruiz, M.; Vincent, T.; Jouannin, C.; Sastre, A. M. *Sep. Sci. Technol.* **2010**, *45*,1935.
41. Zhang, Y.; Kogelnig, D.; Morgenbesser, C.; Stojanovic, A.; Jirsa, F.; Lichtscheidl-Schultz, I.; Krachler, R.; Li, Y.; Keppler, B. K. *J. Hazard. Mater.* **2011**, *196*, 201.
42. Clesceri, L. S.; Greenberg, A. E.; Trussell, R. R., Standard methods for the examination of water and wastewater; American Public Health Association, American Water Works Association, Water Pollution Control Federation: Washington, D.C., **1989**.
43. Tien, C. Adsorption Calculations and Modeling, Butterworth-Heinemann: Newton, MA, **1994**.
44. Juang, R.-S.; Ju, C.-Y. *Ind. Eng. Chem. Res.* **1998**, *37*, 3463.
45. Juang, R.-S.; Lin, H.-C. *J. Chem. Technol. Biotechnol.* **1995**, *62*, 132.
46. Juang, R.-S.; Lin, H.-C. *J. Chem. Technol. Biotechnol.* **1995**, *62*, 141.
47. Liu, Y. *Sep. Purif. Technol.* **2008**, *61*, 229.
48. Ho, Y. S. *Water Res.* **2006**, *40*, 119.
49. Crank, J. The Mathematics of Diffusion, 2nd ed.; Oxford University Press, Oxford, UK, **1975**.
50. Puigdomenech, I. Make equilibrium diagrams using sophisticated algorithms (MEDUSA), Royal Institute of Technology: Stockholm, Sweden, **2013**. Available at: http://www.kth.se/en/che/medusa. Last accessed April 19, 2012.
51. Ruiz, M. O.; Cabezas, J. L.; Escudero, I.; Coca, J. *Chem. Eng. Res. Des.* **2002**, *80*, 537.
52. Belkhouche, N.-E.; Didi, M. A. *Hydrometallurgy* **2010**, *103*, 60.
53. Benamor, M.; Bouariche, Z.; Belaid, T.; Draa, M. T. *Sep. Purif. Technol.* **2008**, *59*, 74.
54. Seddon, K. R.; Stark, A.; Torres, M.-J. *Pure Appl. Chem.* **2000**, *72*, 2275.
55. Fujiwara, K.; Ramesh, A.; Maki, T.; Hasegawa, H.; Ueda, K. *J. Hazard. Mater.* **2007**, *146*, 39.